Revisited Wurtzite CdSe Synthesis : a Gateway for the Versatile Flash Synthesis of Multi-Shell Quantum Dots and Rods

Emile Drijvers,[1,3] Jonathan De Roo,[1,2] Krisztina Fehér,[4] Zeger Hens[1,3] and Tangi Aubert[1,3]

[1] Physics and Chemistry of Nanostructures (PCN), and [2] Sol-gel Centre for Research on Inorganic Powders and Thin films Synthesis (SCRiPTS), Department of Inorganic and Physical Chemistry, Ghent University, Krijgslaan 281-S3, 9000 Ghent, Belgium.

[3] Center for Nano and Biophotonics (NB-Photonics), Ghent University, Sint-Pietersnieuwstraat 41, 9000 Ghent, Belgium.

[4] NMR and Structure Analysis Unit, Department of Organic and Macromolecular Chemistry, Ghent University, Krijgslaan 281-S4, 9000 Ghent, Belgium.

KEYWORDS: Semiconductor, nanocrystal, NMR, CdSe/CdS/ZnS, giant core-shell.

ABSTRACT: Quantum dot core-shell structures are essential to superior optical properties. However, Cd-based quantum dots grown from wurtzite CdSe cores still suffer from irreproducibility due to gel formation during the core synthesis. Moreover, state-of-the-art shelling procedures often remain time consuming. We report here (1) a new procedure of the wurtzite CdSe quantum dot synthesis which eliminates the phosphonic anhydride contamination and (2) the improvement and generalization of the *flash* synthesis for the growth of highly luminescent multi-shell heterostructures. The high versatility of the *flash* procedure enables the epitaxial shelling of wurtzite CdSe by CdS, ZnS and even CdZnS alloys, resulting in a significant enhancement of their photoluminescence efficiency. Thanks to a modification of the CdSe/CdS dot-in-rods synthesis to prevent tip-to-tip connections, the *flash* procedure could also be extended to these anisotropic structures for the growth of multi-shell nanorods as well. The high-quality optical and stability properties of these multi-shell flash heterostructures are of great interest for applications ranging from lighting and displays to long term cell labeling.

Colloidal quantum dots (QDs) have emerged as versatile building blocks for a broad class of applications ranging from photonics to biomedicine.[1-3] The quantum confinement of the excited charge carriers inside semiconductor QDs gives rise to unique size-tunable optical properties. However, surface defects and poor surface passivation with organic ligands can cause trap emission and non-radiative recombination which consequently leads to low photoluminescent quantum yields (PLQY).[4] Furthermore, the undesired single-dot emission intermittency, or ON/OFF blinking, attributed to the non-radiative loss of electron-hole pairs through Auger recombination is often observed in semiconductor QDs.[5, 6] Inorganic materials with larger bandgaps are therefore usually employed to enhance surface passivation and to better insulate the electron-hole pair.[7, 8]

Core-shell structures, such as CdSe/CdS QDs, have been extensively investigated over the last two decades as they offer high photoluminescent quantum yields, narrow and symmetrical emission spectra. In recent years, these heterostructures have increasingly gained attention, with the development of synthetic procedures for the growth of very thick shells. These so-called "giant" core-shell QDs have shown superior optical properties, including high robustness, PLQYs approaching unity and suppressed blinking. These enhanced properties result in part from the large shell volumes but also from other structural characteristics such as alloyed interfaces and high crystallinity.[9-13]

In this context, we recently developed the *flash* synthesis, a method specifically designed for the controllable epitaxial growth of very thick CdS shells within a few minutes of reaction time.[14] These *flash* QDs exhibit high crystallinity and state-of-the-art properties with narrow emission spectra and high PLQY. In addition, Raman spectroscopy revealed an alloyed core/shell interface, resulting in a considerably reduced blinking rate. Thanks to their high quality and robustness, *flash* QDs have already demonstrated their great potential for bioapplications,[15] with lasting optical properties even once encapsulated in a biocompatible silica shell and transferred to water, or for their integration in photonic devices.[16, 17] In spite of this combination of synthetic convenience and high material quality, little efforts have been made to extend seeded-growth approaches beyond CdS shelling of core CdSe QDs. The *flash* synthesis of ZnS and CdZnS shells would, nevertheless, offer a gateway to further optimize the properties of Cd-based core/shell QDs in view of surface passivation, exciton confinement and overall robustness against environmental influences.[18]

Originally, this *flash* synthesis was an adaptation of the method reported by Carbone *et al*. for the synthesis of anisotropic CdSe/CdS dot-in-rods.[19] These nanorods (NRs) constitute another class of interesting materials as they show polarized emission along their long axis, a property of particular interest for lighting and display applications.[19-21] However, these NRs can suffer from tip-to-tip connections. These hamper their large scale ordering, a necessary step to take full advantage of their unique properties in, for example, display applications.[22]

Our early findings quickly indicated that these connections would be equally detrimental for the growth of a ZnS shell in a subsequent step.

In the past few years, one of the key parameter that allowed for the synthesis core-shell QDs and NRs with excellent optical properties has been the development of syntheses at elevated temperatures (typically over 300 °C).[11, 12, 14, 19] One can indeed reasonably expect that this produces materials with higher crystallinity. Diroll *et al*. have notably reported that core-shell structures synthesized at higher temperature show optical properties with enhanced robustness and thermal stability.[23] At those temperatures, only the wurtzite crystal structure is stable. Thus, since the synthesis of such core-shell structures relies on a seeded epitaxial growth, it therefore requires the synthesis of wurtzite CdSe QDs beforehand. As it happens, many of the above mentioned heterostructures start from the same wurtzite CdSe QD synthesis.[11, 12, 14, 19] This particular synthesis makes use of a phosphonic acid for the complexation of the cadmium precursor and stabilization of the QDs. However, the formation of a phosphonic anhydride, during this synthesis has already extensively been addressed.[24-27] This by-product is rather insoluble at lower temperatures and its elimination still remains a challenge. Indeed, this phosphonic anhydride typically causes a gelification of the QD suspension, which is a strong limitation for their use in the subsequent synthesis of high quality core-shell QDs, as well as for the upscaled production of these QDs.

Here, we develop a generic, multiple *flash* approach for the formation of a diversity of Cd-based core/shell QDs and NRs. To achieve this, we first tweak the original wurtzite CdSe QDs synthesis to prevent the phosphonic anhydride formation by adding a long chain alcohol to the reaction. This reproducibly yields larger amounts of QDs with higher purity and we provide herein a detailed description of their novel surface chemistry through nuclear magnetic resonance (NMR) spectroscopy. From these cores, we introduce a standardized *flash* synthesis of high quality core-shell QDs. We show that the purity of the core materials is key to obtain core-shell QDs with optimal properties. This is evidenced through the synthesis of CdSe/CdS QDs with enhanced optical properties. We thereafter demonstrate that the *flash* procedure can be conveniently extended to the growth of ZnS and alloyed CdZnS layers, resulting in multi-shell QDs with even higher PLQYs. In view of the synthesis of multi-shell NRs we also modified the dot-in-rod synthesis in order to prevent the tip-to-tip connections observed between rods, simply by changing the length of the short-chained phosphonic acid. Thanks to this modification of the original dot-in-rod synthesis, we demonstrate how the standardized *flash* procedure can also be applied to these anisotropic structures for the synthesis of CdSe/CdS/ZnS NRs. We thus conclude that the standardization of this *flash* procedure presented here constitutes an essential step towards the large scale production of these materials, regardless of the grown material.

EXPERIMENTAL SECTION

Materials. CdO (≥99.99%), oleyl alcohol (OlOH, 85%) and ZnO (99.999%) were purchased from Sigma-Aldrich. N-octadecylphosphonic acid (ODPA, ≥97%), n-tetradecylphosphonic acid (TDPA, ≥97%) and n-dodecylphosphonic acid (DDPA, ≥97%) were purchased from PlasmaChem GmbH. Trioctylphosphine (TOP, ≥97%) and sulfur (S, 99.999%) were purchased from Strem Chemicals. Trioctylphosphine oxide (TOPO, for synthesis) was purchased from Merck Millipore while selenium powder (Se, -200 mesh, 99.999%) and oleic acid (OA, 90%) from Alfa Aesar. Toluene, methanol and chloroform were purchased from Fiers. The stock solutions of TOP-Se (1.7 M) and TOP-S (2.4 M) were prepared by dissolving 1.343 g of the selenium powder and 0.7704 g of sulfur in 10 mL of TOP respectively. Toluene d^8 (99.5% deuterated) was purchased from Euriso-top.

Synthesis of the wurtzite CdSe core QDs. This new wurtzite CdSe QDs synthesis was adapted from the previously reported procedure in literature.[19] 1.5 mmol (0.1925 g) of CdO, 6 mmol (1.670 g) of n-tetradecylphosphonic acid (TDPA), 24 mmol (6.44 g) of oleyl alcohol (OlOH) and 10 g of trioctylphosphine oxide (TOPO) were mixed in a 50 mL three-neck flask. The mixture was heated to 150 °C under nitrogen atmosphere for one hour. The solution was then heated to 350 °C. 2 mL of trioctylphosphine (TOP) was injected as soon as the solution became colorless, indicating the dissolution of CdO. Once the mixture reached 350 °C, 2.55 mmol (1.5 mL) of a 1.7 M trioctylphosphine selenide (TOP-Se) solution was injected. After a reaction time of typically few seconds to few tens of seconds depending on the envisaged QD size, the reaction was quenched by a sudden drop in temperature using a water bath pre-heated to 80°C to avoid cracking of the flask. Once the temperature of the mixture reached 80 °C, 20 mL of methanol was injected in the flask to precipitate the QDs. The mixture was then centrifuged at 4000 rpm for 1 minute. The supernatant was discarded and the QDs were purified three time with toluene and methanol as solvent and non-solvent. The QDs were dispersed and stored in 3 mL toluene. Overnight, the possible and very limited solid formation was removed by centrifuging the sample. The size of the QDs was determined from the position of the first excitonic absorption peak using the sizing curve of Mulvaney *et al.*.[28] The concentration of the wurtzite CdSe dispersion was determined based on their absorbance at 300 nm and 350 nm in toluene using the corresponding intrinsic absorption coefficients of wurtzite CdSe (μ_{300} = 244046 cm^{-1} and μ_{350} = 130823 cm^{-1}) calculated from the Maxwell–Garnett effective medium theory.[29, 30] As in the original synthesis described by Carbone *et al.*,[19] the size of the CdSe QDs is adjusted by controlling the reaction time. Nevertheless, one should note that for QDs sizes below 3 nm, reaction times of no more than a few seconds are required, which can be hard to achieve and with poor size reproducibility. Thus, in those case it is more efficient to use the volume of oleyl alcohol to quench the reaction, *i.e.* the oleyl alcohol is not initially present in the reaction flask but injected after the reaction time, which result in a very fast and reproducible quenching. In our experiments, this always led to the same results regarding the purifications of these QDs. In order to facilitate the comparison of their optical properties, all the QDs and NRs reported here were prepared starting from 3 nm CdSe cores, *i.e.* synthesized with the oleyl alcohol already present in the reaction flask.

***Flash* Synthesis of Multi-Shell Quantum Dots.** The versatile *flash* synthesis can be applied for the growth of different shell materials, such as CdS, ZnS and even alloyed CdZnS. For all shell growths, 2.5 g of oleic acid (OA) and 5 g of TOPO were added to a three-neck flask together with CdO and/or ZnO, for the respective growth of the desired material. The amounts of CdO and/or ZnO were calculated based on the envisaged shell thickness, considering a full anionic chemical yield, and with a

molar excess of 1.2 of the cation compared to the anion. The thicknesses of the shells can hence be tuned by varying the amounts of CdO and/or ZnO. The mixture was heated to 150 °C under nitrogen atmosphere for one hour. The solution was then heated to 350 °C where 1 mL of TOP was injected as soon as the solution became colorless, indicating the dissolution of CdO and/or ZnO. After the temperature recovered, a solution was injected, containing the seed QDs (*i.e.* either CdSe or CdSe/CdS QDs depending on the synthesis step), trioctylphosphine sulfide (TOP-S, 2.4 M) of which the volume was always adjusted to 2 mL with TOP, to account for the same temperature drop. The amount of seeds injected for the shell growth varied depending on the synthesis step. Typically, the first shell growth was executed on 200 nmol of seeds while the subsequent shell growths were executed on 15 nmol then on 5 nmol of seeds. After 5 minutes, the reaction was quenched by a sudden drop in temperature using a pre-heated water bath. Once the mixture has cooled down to room temperature, the QDs were precipitated by adding 10 ml of methanol and 2 ml of toluene to ensure miscibility of the mixture. The QDs were collected by centrifugation at 4000 rpm for 3 min and further purified twice with toluene and methanol as solvent and non-solvent. The QDs were dispersed and stored in toluene. After each shell growth, the size of the QDs was determined by TEM analyses. In the case of QDs with only CdS shells their concentration was determined based on their absorbance in toluene at 300 nm and 350 nm using the corresponding intrinsic absorption coefficients of the CdSe/CdS calculated from the Maxwell–Garnett effective medium theory depending on the ratio between the CdSe core and CdS shell volumes.[29, 30] For QDs with either ZnS and/or CdZnS shells, there is not yet a consistent model to determine the intrinsic absorption coefficients of such complex heterostructures. In those cases, the concentrations were estimated from the amount of seeds involved in the reaction to which 10% were subtracted to account for the QDs lost in the reaction and purification steps.

***Flash* Synthesis of Multi-Shell Nanorods.** Firstly, CdSe/CdS dot-in-rods were grown from the wurtzite CdSe seeds, following the method of Carbone *et al.*,[19] which was slightly modified for further improvement of these NRs. For all syntheses, 5 g of TOPO was added to a three-neck flask, with a varying amount of octadecylphosphonic acid (ODPA), dodecylphosphonic acid (DDPA) and CdO, depending on the desired diameter and length of the NRs. The total amount of phosphonic acid to Cd molar ratio was of 3:1, while the molar ratio ODPA to DDPA was of 1.5:1. The mixture was heated to 150 °C under nitrogen atmosphere for one hour. The solution was then heated to 350 °C where 1 mL of TOP was injected as soon as the solution became colorless, indicating the dissolution of CdO. After the temperature recovered, a solution was injected, containing the CdSe seeds, TOP-S (2.4 M) and whose volume was always adjusted to 2 mL with TOP to account for the same temperature drop. In this case, the rods were grown from 50 nmol of CdSe seeds. Similarly to the growth of CdS shells on spherical QDs, the molar ratio Cd to S was of 1.2:1 to ensure a cation rich surface. The reaction was quenched after 8 minutes using a pre-heated water bath. Precipitation of the NRs was achieved by injecting 5 ml of toluene and 10 ml of methanol when the mixture had reached 120 °C and 80 °C respectively. The NRs were then immediately collected by a short centrifugation step of 1 min at 4000 rpm. Longer centrifugation durations or a lower temperature of the mixture would typically result in the precipitation of a phosphonic anhydride polymer that would hardly be separable from the NRs and should therefore be avoided. The NRs were further purified twice with toluene and methanol as solvent and non-solvent. Finally the NRs were dispersed and stored in toluene. The growth of a ZnS shell on the CdSe/CdS dot-in-rods was performed with the same procedure described in the previous paragraph for spherical QDs, using typically 10 nmol of NRs. The dimensions of the NRs were systematically determined by TEM observations. In the case of purely CdSe/CdS NRs, the concentrations were determined from the absorbance at 300 nm and 350 nm, by considering that only the very large volume of wurtzite CdS contributes to the absorption at these wavelengths, and using its intrinsic absorption coefficients (μ_{300} = 173021 cm^{-1} and μ_{350} = 118769 cm^{-1}) calculated from the Maxwell–Garnett effective medium theory,[29, 30] and considering the NRs as cylinders. In the case of NRs with a ZnS shell, the concentration were estimated from the amount of seeds involved in the reaction to which 10% were subtracted to account for the NRs lost in the reaction and purification steps.

Material characterization. Bright field transmission electron microscopy (TEM) images and energy-dispersive x-ray spectroscopy (EDX) measurements were made using a Cs-corrected JEOL 2200FS microscope. Absorption spectra were taken using a Perkin Elmer Lambda 950 spectrometer. Photoluminescence measurements were done on an Edinburgh Instruments FLSP920 UV−Vis−NIR spectrofluorimeter. For steady-state measurements, a 450 W xenon lamp was used as the excitation source. All steady-state emission spectra were recorded for an excitation wavelength of 365 nm and were corrected for the detector sensitivity. The PLQYs were measured by using an integrating sphere, with an improved method adapted from Mello *et al.*[31] in order to correct the measurements for internal reflections.[15] The time-resolved measurements were performed using a picosecond pulsed LED (331 nm, bandwidth 9.4 nm, pulse width 872 ps) as the excitation source, and collecting the signal at the maximum of emission (bandwidth 10 nm). Lifetimes were calculated by fitting the first 90% of the photoluminescence (PL) decay traces with a single exponential function (Equation 1):

$$R(t) = e^{(-t/\tau)} + A \qquad [1]$$

With A being a constant to account for the long tail of some decays. Results of the fits always gave χ^2 values below 1.15. Nuclear magnetic resonance (NMR) samples were prepared by drying the purified QDs dispersion with a nitrogen flow which were then redispersed in 500 µL deuterated toluene and inserted in a 5 mm tube. The sample temperature was set to 298.15 K. NMR measurements were recorded on a Bruker Avance III spectrometer operating at a ^{1}H frequency of 500.13 MHz and equipped with a BBI-Z probe. Quantitative ^{1}H spectra were recorded with a 30 s delay between scans to allow full relaxation of all NMR signals and the 1D spectra were multiplied with an exponential window function. The quantification was done by using the Digital ERETIC method. Diffusion measurements (2D DOSY) were performed using a double-stimulated echo sequence for convection compensation and with monopolar gradient pulses.[32] Smoothed rectangle gradient pulse shapes were used throughout. The gradient strength was varied linearly from 2 to 95% of the probe's maximum value (calibrated at 50.2 G/cm) in 64 steps, with the gradient pulse duration and diffusion delay optimized to ensure a final

attenuation of the signal in the final increment of less than 10% relative to the first increment. The alkene and methyl proton resonances were corrected prior to integration by subtracting a linear background from the measured intensity. The diffusion coefficients were obtained by fitting the appropriate Stejskal−Tanner equation (Equation 2) to the signal intensity decay.[33]

$$I = I_0\, e^{[-D\gamma^2 g^2 \delta^2 (\Delta - 0.6\delta)]} \qquad [2]$$

Two-dimensional ^{1}H NOESY (nuclear Overhauser effect spectroscopy) spectra were acquired using a standard pulse sequence from the Bruker library, noesygpphpp. NOESY mixing time was set to 300 ms and with 4096 data points set in the direct dimension and 512 data points set in the indirect dimension. For 2D processing, before Fourier transformation, the 2D spectra were multiplied with a squared sine bell function in both dimensions. ^{1}H - ^{13}C HMBC (Heteronuclear Multiple-Bond Correlation) and ^{1}H – ^{31}P HMQC (Heteronuclear Multiple Quantum Correlation) spectra were acquired using standard pulse sequences from the Bruker library, hmbcgplpndqf and hmqcgpndqf respectively. The delays were set to long range $^nJ^1_H{}^{13}_C$ and $^nJ^1_H{}^{31}_P$ couplings of 8 Hz and 12 Hz in the ^{1}H - ^{13}C HMBC and ^{1}H – ^{31}P HMQC respectively, while the one bond $^1J^1_H{}^{13}_C$ couplings of 145 Hz were filtered out in the ^{1}H - ^{13}C HMBC.

RESULTS AND DISCUSSION

Revisited Synthesis of the Wurtzite CdSe Quantum Dots. Cadmium phosphonate precursors are usually used in the synthesis of wurtzite CdSe QDs. However, phosphonic acids are prone to polymerization[24-27] and this leads to the precipitation of part of the QD dispersion after synthesis and/or during purification. This is illustrated in **Figure 1a** which shows an image of a partially solidified CdSe QD dispersion due to the presence of a insoluble phosphonic anhydride. This is a serious limitation which also compromises the chemical yield of the synthesis and points in general to a poorly controlled ligand shell and hence limited colloidal stability. Moreover, core-shell QDs grown from these solidified cores typically show poor structural morphology, see **Figure 1b**. We have found that for small scale reactions, some purification methods such as a precipitation and centrifugation at elevated temperatures or the repeated purification of the QDs with a short chain amine, could partially remove the phosphonic anhydride. However, these techniques do not show satisfying results for larger scale reactions. Although problematic, the phosphonate precursor seems difficult to replace considering the high temperatures (over 300 °C) that are required to ensure a high quality wurtzite structure. For instance, using a cadmium oleate precursor at those temperatures results in reactions too fast to control, yielding QDs with diameters persistently exceeding 5 nm.

In chemical terms, the issue with the wurtzite CdSe QDs synthesis appears well understood. The excess phosphonic acid and cadmium phosphonate in the reaction mixture can readily react to form a phosphonic anhydride polymer, **Figure 2c**. This anhydride polymer precipitates with the nanocrystals during centrifugation, compromising the purification of the QDs. There is a possibility that the tightly bound phosphonate also reacts via its remaining free hydroxyl group to form the anhydride.

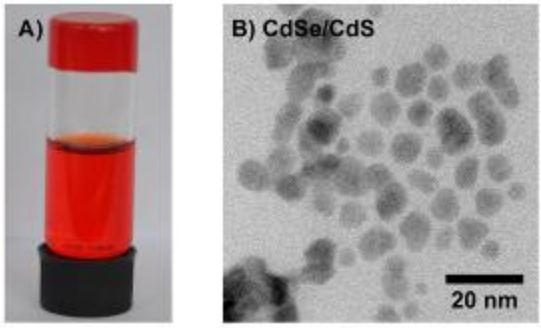

Figure 1. a) Image of an upside down vial containing wurtzite CdSe QDs synthesized with the method described in the literature,[19] with the solidified fraction still attached to the bottom of the vial. b) TEM image of core-shell QDs grown from the solidified CdSe cores which result in particles with poor structural morphology.

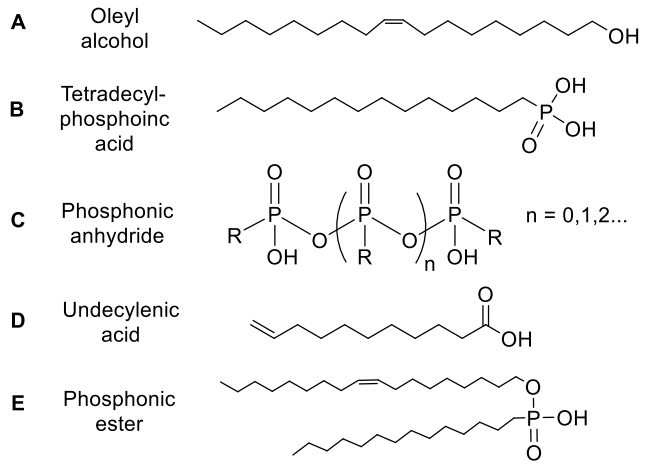

Figure 2. Molecular structures of a) oleyl alcohol (OlOH), b) tetradecylphosphonic acid (TDPA), c) a phosphonic anhydride, d) undecylenic acid and e) a phosphonic ester.

Use of oleyl alcohol (OlOH). In order to prevent the formation of this phosphonic anhydride, we decided to use a mixture of OlOH and phosphonic acid to dissolve the CdO and thus prepare the actual cadmium precursor. By this approach, the alcohol and the phosphonic acid form a phosphonic ester, which only contains one hydroxyl group, see **Figure 2e**. By removing one hydroxyl group through ester formation, this strategy avoids the condensation of the phosphonic anhydride polymer, which seems to be confirmed by the lack of precipitates or gels upon purification of the QDs using classical solvent-nonsolvent procedures. Up to now, octadecylphosphonic acid (ODPA) was the phosphonic acid of choice in the wurtzite CdSe synthesis. Here, we substituted it for tetradecylphosphonic (TPDA) as the resulting phosphonic ester between ODPA and OlOH proved to be insoluble, opposite from the respective TDPA ester.

Solution ^{1}H and ^{31}P NMR analysis was subsequently employed to characterize the surface of the wurtzite CdSe QDs and confirm the presumed role of OlOH. According to the sole occurrence of a broadened CH_3 resonance (**Figure 3a**, around 1 ppm), the dispersion is sufficiently purified and only bound ligands are present.[34] However, both TDPA and OlOH have a CH_3 resonance, rendering it impossible to distinguish both species by this resonance. In contrast, only OlOH has an alkene resonance at 5.5 ppm, which makes it easily identifiable

in the ^{1}H NMR spectrum. In addition, this resonance is broadened, confirming the interaction of OlOH with the CdSe surface. Diffusion NMR (DOSY) measurements were carried out and by fitting the diffusion decay to the appropriate Stejskal–Tanner equation,[33] the diffusion coefficient was determined (**Figure 3b**). For both the CH_3 and the alkene resonance, we find a diffusion coefficient of 105 µm²/s, which is converted by the Stokes-Einstein equation to a solvodynamic diameter of 7 nm. This size is consistent with a nanocrystal size of 3 nm – as determined from the wurtzite CdSe sizing curve – and an organic capping layer of 2 nm. This shows that both OlOH and TDPA diffuse together with the QDs and are thus tightly bound to the QD surface. Although this feat is not unsurprising for a strong X-type ligand as TDPA, it is unlikely for OlOH since alcohols were found very weak L-type ligands, typically exchanging fast between a free and a bound state.[35] Therefore, we propose that OlOH has formed a phosphonic ester with TDPA (**Figure 2e**), which is bound to the CdSe surface in its deprotonated form.

To support these conjectures, we sought to strip the surface ligands from the surface. Although carboxylic acids are too weak an acid to displace phosphonic acids,[36] it was shown before that amines can promote the exchange of a stronger acid for a weaker one.[37-39] Therefore, we added a large excess of undecylenic acid and butylamine to the QD dispersion and analyzed the exchanged species *in-situ* in the NMR tube, see **Figure 3a**. Undecylenic acid has a terminal alkene and consequently features two resonances in the alkene region, one at a slightly lower and one at a slightly higher chemical shift compared to the internal alkene resonance of OlOH. As a result of the stripping, sharp resonances appear in the ^{1}H NMR spectrum at around 5.5 and 4 ppm, suggesting that the molecules associated with those resonances are no longer bound to the QDs. Indeed, the NOESY spectrum clearly confirms that these molecules are not interacting with the surface since the sharp resonances feature positive (red) NOEs (as defined by an opposite sign of the cross peak to the diagonal), indicated by the arrows, **Figure 3c**. The resonance at 4 ppm is particularly interesting since this is the typical region for the α-CH_2 of an alcohol that has reacted to form an ester (resonance 2). In order to distinguish between the phosphonic ester of OlOH and TDPA or the ester of OlOH and undecylenic acid, ^{1}H–^{31}P HMQC and ^{1}H–^{13}C HMBC spectra were recorded. The ^{1}H–^{31}P HMQC (**Figure 3d**) revealed a coupling between resonance 2' and a phosphorous nucleus, suggesting a phosphonic ester. In contrast, correlations with carbons are absent in the ^{1}H–^{13}C HMBC spectrum (**Figure 3e**), excluding regular esters. Quantitative ^{1}H NMR analysis indicates that the total ligand density of the wurtzite CdSe QDs amounts to 3.9 ligands/nm^2, with phosphonic esters representing 25% and TDPA 75% of this total.

We thus conclude that the addition of OlOH eliminates (part of) the hydroxyl groups of the phosphonic acid by forming a phosphonic ester. This suppresses the tendency to form phosphonic anhydride polymers. The addition of OlOH also maintains the excess cadmium phosphonate in a liquid state even at room temperature, allowing their convenient separation by centrifugation. This modification in the wurtzite CdSe synthesis has made it possible to upscale the reaction to yield up to over a significant 1.5 µmol (≈ 150 mg) of QDs produced in a single reaction. Thanks to their high purity this large amount of QDs could be stored at high concentration, dispersed in only a few mL of toluene.

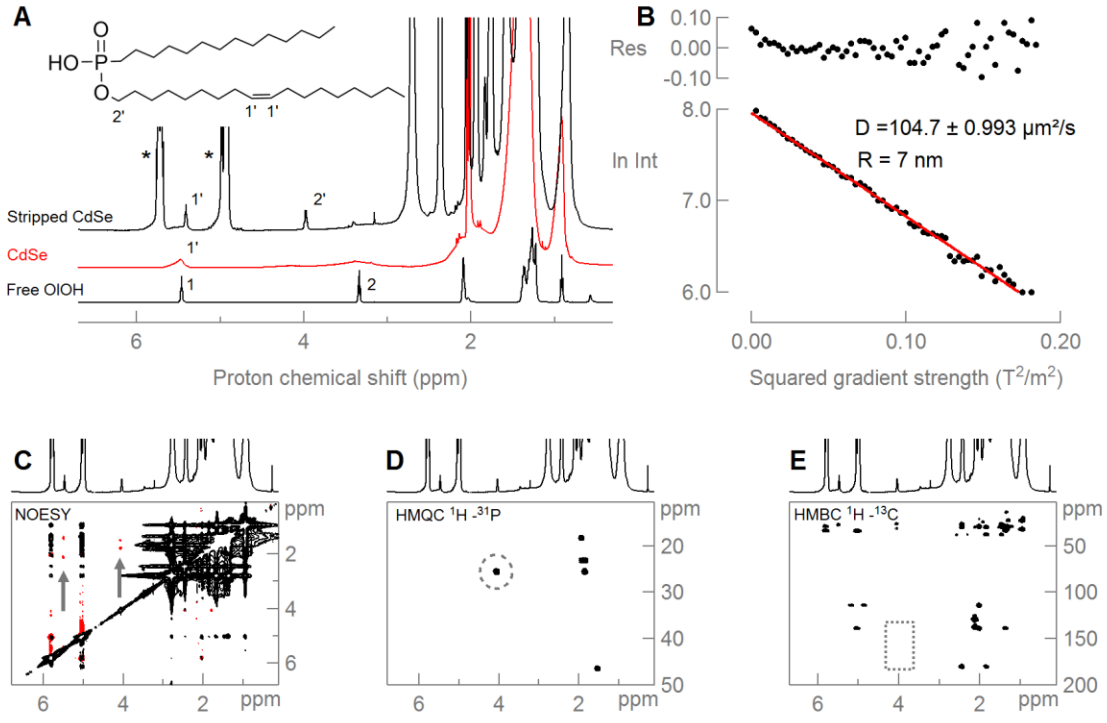

Figure 3. a) ^{1}H NMR of the free oleyl alcohol (bottom), CdSe QDs (middle) and of the *in-situ* stripped surface ligands of the CdSe QDs with undecylenic acid and butylamine (top) all in deuterated toluene. (1) Alkene and (2) CH2 resonances of the oleyl alcohol free in solution. (1') Alkene resonance and (2') the alfa CH2 of the alkoxy chain of phosphonic ester. (*) Alkene signals of undecylenic acid in large excess. b) DOSY mono-exponential decay of the alkene resonance on the bound phosphonic ester. c) NOESY, d) ^{1}H-^{31}P HMQC and e) ^{1}H-^{13}C HMBC) spectra of the stripped phosphonic ester. The arrow points at the resonances of the exchanged phosphonic ester, while dashed circle confirms the presence of the phosphonic ester and the dashed rectangle excludes regular esters.

The *Flash* Synthesis for Multi-Shell Quantum Dots. A series of modifications have been made to the *flash* procedure compared to the previously reported method.[14] This involves the optimization and standardization of the process, geared towards the growth of different shells and an overall improvement of the quality of the resulting materials. The reaction time was extended from 3 to 5 min. Although after 3 min the final size is already reached, even in the case of very thick shells, a reaction time of 5 min was found to yield somewhat more spherical QDs without affecting their size dispersion. This is often preferred in further application of these QDs but also for a more accurate concentration determination since the latter is calculated based on the volume of the QDs. A 1.2 cationic excess was used instead of an anionic excess in previous *flash* procedure, as this was found not to affect the quality of the QDs and to achieve optimum passivation of the outer surface. The amount of seeds was significantly upscaled from 87 nmol to 200 nmol. Besides being an important step towards applications of these materials, larger scale syntheses at higher concentrations were also found to improve the size dispersion of the obtained QDs. A fixed amount of 2.5 g of oleic acid was chosen rather than a varying Cd:OA ratio approach. Indeed, in the case of thin shells, the amount of oleic acid added to the reaction using a ratio approach can be too small to compete with the residual phosphonic acids on the core QDs, resulting in the growth of rod-like QDs. In the case of very thick shells, the amount of injected cores can be limited to 100 nmol so as to keep the Cd:OA ratio above 1:3; a value we found is the lower limit to ensure full dissolution of the CdO and a proper shelling. Finally, the reaction temperature was increased from 330 to 350°C in order to homogenize all protocols for isotropic and anisotropic shells. In addition, it was reported that syntheses of such core-shell structures at higher temperatures typically yield materials with enhanced and more robust optical properties.[23]

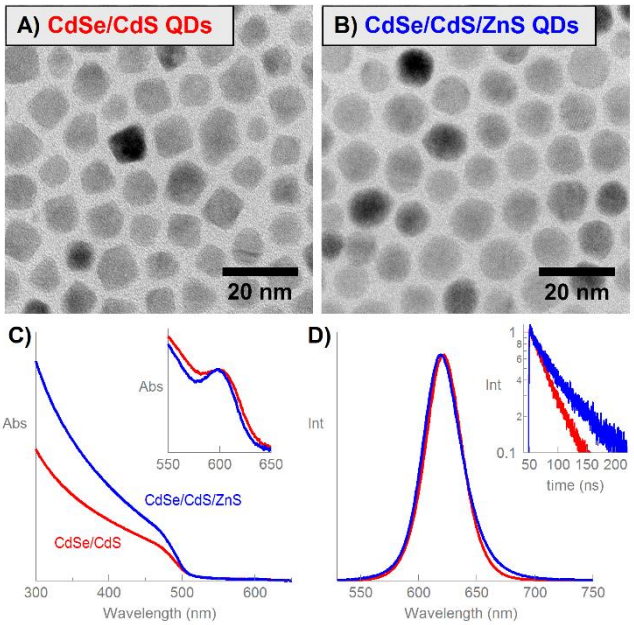

Figure 4. TEM images of a) CdSe/CdS and b) CdSe/CdS/ZnS QDs. Optical properties with c) normalized absorption spectra (inset: focus on the excitonic feature at 600 nm), d) normalized emission spectra (inset: normalized photoluminescence decays of the QDs).

CdSe/CdS QDs. Figure 4a shows an example of 9.1 nm CdSe/CdS QDs obtained from this new *flash* procedure (see the Supporting Information, **Figure S1**, for more sizes). These QDs show good morphology with a size dispersion below 15%, which is the case for all the QDs reported here. One should note that size dispersions below 10% can still be achieved by further increasing the concentration of the seeds in the *flash* synthesis (see the Supporting Information, **Figure S2**). Moreover, the CdSe/CdS QDs obtained from this modified *flash* procedure feature improved optical properties, which are reported in **Figure 4c-d** for the example of the 9.1 nm CdSe/CdS QDs shown in **Figure 4a**. As expected for such large core-shell structures, the absorption spectrum is mostly characterized by a featureless bulk-like CdS absorption below 500 nm, although the excitonic feature is still clearly identifiable at around 600 nm (inset **Figure 4c**). The emission spectrum is centered at 622 nm with a full-width half-maximum (FWHM) of only 37 nm. Furthermore, these *flash* CdSe/CdS QDs show a high PLQY of 72%. Another evidence of the good quality of these CdSe/CdS QDs is their PL decay, inset **Figure 4d**, which can be fitted well to a single exponential (resulting in a lifetime of τ = 35.1 ns). The absence of a fast component in the PL decay, which would be characteristic of non-radiative processes, is in line with the high PLQY. The enhanced quality of these *flash* CdSe/CdS QDs compared to previous generation can be attributed in large part to the higher purity of the CdSe cores. Indeed, the wurtzite CdSe cores synthesized with this new synthetic protocol making use of oleyl alcohol are not only suitable for the growth of a CdS shell in spite of their slightly different surface chemistry, they also promote the growth of a much more homogeneous shell.

CdSe/CdS/ZnS QDs. Multi-shell QDs can be synthesized through a double *flash* method. An additional ZnS layer is grown on the core-shell QDs with virtually no change to the procedure except for replacing the CdO for ZnO in the reaction (see experimental section). **Figure 4** shows the TEM images of corresponding CdSe/CdS and CdSe/CdS/ZnS QDs. EDX analyses confirmed the presence of Zn in the CdSe/CdS/ZnS QDs (13 % relatively to the overall composition). However, in spite of aiming at a 3 nm thick layer in the calculations for the synthesis of the ZnS shell, the TEM analyses reveal that the diameter only increases from 9.1 nm to 10.2 nm. This corresponds to 1 to 2 monolayers of ZnS and is in line with the fraction of Zn as measured by EDX. All attempts to increase the thickness of the ZnS shell by either increasing the reaction time, increasing the amount of precursors, varying the temperature and seed concentration or even trying a multi-step growth never yielded thicker ZnS shells. In addition the thickness of the obtained ZnS layer was found to be relatively independent of the size of the CdSe/CdS QDs as illustrated in the Supporting Information, **Table S1**. This saturation limit in growth can most likely be explained by the lattice mismatch of about 8% between the wurtzite CdS and wurtzite ZnS structures, whereas the mismatch between the wurtzite CdSe and wurtzite CdS structures is only about 4%. The TEM images in **Figure 4** also evidence that the QDs fully retain their size dispersion after a second *flash* procedure.

Moreover the QDs appear to have an even more spherical shape.

Regarding the optical properties of these CdSe/CdS/ZnS QDs, they are compared systematically with those of the corresponding CdSe/CdS QDs in **Figure 4c-d**. From point of view of absorption (**Figure 4c**), when normalizing the spectra at the maximum of the first exciton absorption, the growth of the ZnS shell translates into an increase in absorption at energies even below the bulk band-gap of ZnS (3.91 eV). It is also characterized by a more pronounced dip in the absorption spectrum after the first exciton transition (inset **Figure 4c**). The position of the emission peak on the other hand features a slight, 2 nm blue-shift (**Figure 4d**), something we consistently found for other QD sizes, except for very thin CdS layers (see the Supporting Information, **Table S1**). The most pronounced effect of the ZnS shell growth is found in the PL decay (inset **Figure 4d**) as it increases the lifetime from 35.1 ns in the case of the CdSe/CdS QDs to 53.0 ns for the CdSe/CdS/ZnS QDs. Although the PL decay of the CdSe/CdS/ZnS QDs seems to deviate from a pure single exponential, it is due to a long tailing rather than to a fast component that would be due to non-radiative processes. In the measurements, this long tailing is better fitted by including a constant in the fit function (see experimental section) than by adding a second exponential. This could be the sign of delayed emission due to the existence of long-lived charge-separated states as it was already reported for similar structures.[40] Finally the PLQY increases from 72% to 74%, which is in line with a better passivation and confinement thanks to the larger band-gap of ZnS. Even though the increase in PLQY might seem limited, this actually confirms the good quality and passivation of the starting CdSe/CdS QDs, which is already reflected in their high initial PLQY. Nevertheless, this increase was much more pronounced in the case of large QDs which have a lower PLQY to start with (see the Supporting Information, **Table S1**).

Similar changes in the optical properties of the QDs, including the blue-shift in emission as well as the increase in lifetime after the growth of a ZnS shell on CdSe/CdS QDs, were already reported by Boldt *et al.*[18] In their synthesis, the ZnS grows progressively owing to a rather slow continuous injection of the Zn and S precursors. They first observe a blue-shift at early stages of the shell growth, followed by a red-shift as the ZnS shell kept growing. These authors attributed the blue-shift to an alloying between the CdS and ZnS shells, causing an increase in the confinement of the excitons, and the subsequent red-shift to an alloying between the CdSe core and the CdS due to the longer reaction time, resulting in a quasi-type II core-shell structure. They further support this claim with the increase in the lifetime after longer reaction time. However, their conclusions are somewhat contradictory with the observation made here in the case of a very fast and limited growth of a ZnS shell. In our case, both the blue-shift and the increase in lifetime are observed concomitantly. The blue-shift therefore cannot be explained by an increased confinement as this could only result in a better overlap of the electron and hole wave functions and in a decrease of the lifetime. This was evidenced by Diroll *et al.*[41] who modified the method of Boldt *et al.* for the synthesis of CdSe/CdZnS dot-in-rods and clearly showed the lifetime decrease with a proper alloying of CdS and ZnS. Furthermore, here the blue-shift in emission is also observed for QDs with very large sizes where slight change in the confinement is not likely to have any influence on the optical properties, whereas we actually observe a red-shift for small sizes which should be much more sensitive to changes in the confinement (see the Supporting Information, **Table S1**). Although we cannot fully explain this discrepancy, the additional strain generated by the growth of the ZnS with a large lattice mismatch may affect the electronic structures of the QDs. Indeed, strain generated piezoelectric fields have been reported to becomes significantly important in such large non-centrosymmetric CdSe/CdS core-shell structures.[42]

CdSe/multiCdS QDs. One of the challenges when growing QDs with very thick shells is to maintain their brightness. Indeed, while the PLQY of the QDs initially increases with the thickness of the CdS shell, it then typically decreases when reaching shells over 5 nm in thickness (see the Supporting Information, **Table S1** for illustration). This is most likely due to increased strain in the structure but also due to the presence of QDs with poor morphology as highlighted in **Figure 5a**. The shape of those QDs sometimes even suggests that they could consist of several CdSe cores into a single structure, which would have dramatic consequence for the PLQY. Indeed, the proximity of cores within the same shell would favor energy transfer between them and increase non-radiative recombination rates. The *flash* synthesis offers an alternative to this limitation as multiple CdS shells can be grown on top of each other in successive *flash* procedures. **Figure 5a** shows for instance the TEM images of 14.7 nm CdSe/CdS QDs grown in a single step and **Figure 5b** shows 15.8 nm CdSe/CdS QDs where the CdS shell was grown in 3 successive steps, and therefore denoted CdSe/3.CdS. These CdSe/3.CdS QDs were grown from initially 8.5 nm sized CdSe/CdS QDS, hence highlighting that in this case the growth in multi-step is not limited as in the case of ZnS shells. As the CdSe/3.CdS QDs show good morphology without any of the poor quality QDs visible in the large CdSe/CdS sample, it is also characterized by a PLQY of 64% which is considerably better than the 23% of the CdSe/CdS QDs in **Figure 5a**. Furthermore, these CdSe/3.CdS QDs show a 140-fold increase between their absorption coefficient at the first excitonic peak and at 450 nm. A property which is of high importance to prevent self-absorption when using QDs in solar concentrators for instance.[43, 44]

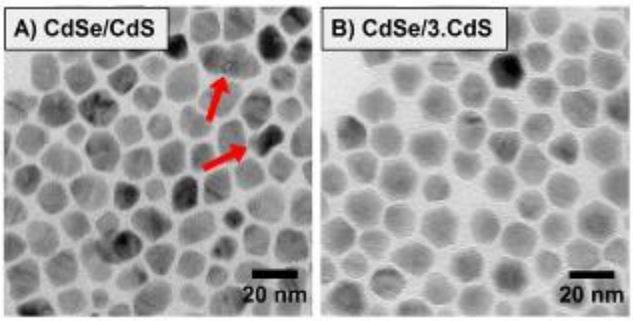

Figure 5. TEM images of a) CdSe/CdS QDs grown in a single step, and b) CdSe/3.CdS QDs grown in multiple steps. Red arrows in a) to highlight QDs with poor morphology.

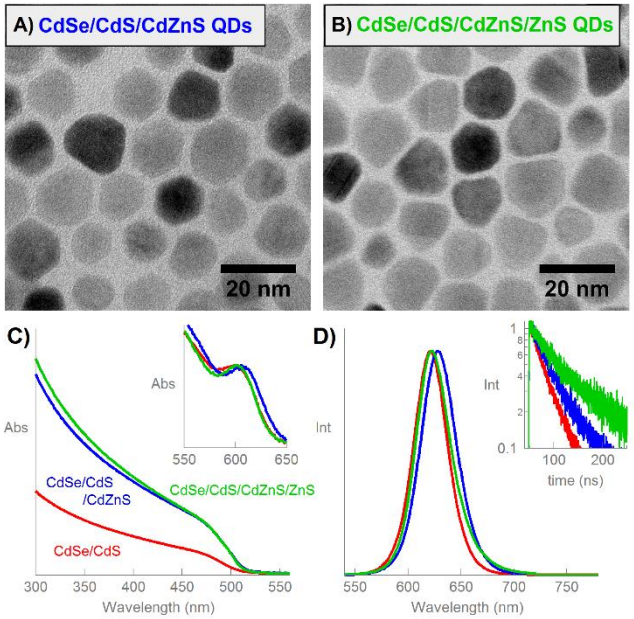

Figure 6. TEM images of a) CdSe/CdS/CdZnS and b) CdSe/CdS/CdZnS/ZnS QDs. Optical properties with c) normalized absorption spectra (inset: focus on the excitonic feature at 600 nm), d) normalized emission spectra (inset: normalized photoluminescence decays of the QDs).

Alloyed CdZnS shells. The high versatility of the *flash* method is further demonstrated through the growth of alloyed CdZnS shells. As described in the experimental part, this is simply achieved by mixing CdO and ZnO in the reaction flask prior to injection of the seed QDs and sulfur precursor. All the parameters for the growth of such alloyed shells remain identical as for the growth of a CdS or ZnS shell. **Figure 6a** shows the TEM image of CdSe/CdS/CdZnS QDs of 12.3 nm in size grown from the same 9.1 nm CdSe/CdS QDs as shown in **Figure 4a**. It corresponds to the growth of a 1.6 nm thick shell, in spite of aiming at a 3 nm thick shell in the synthesis calculations. In addition, the synthesis was made with a molar ratio of 75% Zn for 25% Cd, whereas EDX analyses revealed that the additional shell only contains 15% Zn (relatively to the cations composition). This lower amount of Zn compared to the theoretical ratio in the reaction mixture is line with the growth of a thinner shell and can be reasonably explained by either a lower reactivity of the Zn precursor and the limited growth of a pure ZnS shell even after all the Cd has reacted for the same reason as for CdSe/CdS/ZnS QDs. Thus, although this was not investigated in details, it is more likely that the CdZnS shell is not made of a homogeneous alloy of Cd and Zn, but rather features a gradient composition with increasing Zn content towards the QD surface. Indeed, when attempting to further grow an additional 3 nm thick ZnS shell on top of these CdSe/CdS/CdZnS QDs, the QDs did not grow significantly in size. **Figure 6b** shows the TEM image of CdSe/CdS/CdZnS/ZnS QDs obtained with a triple *flash* procedure, which were also measured to have an average diameter of 12.3 nm. Nevertheless, EDX analyses showed an increase of the Zn content, from 15% in the CdZnS shell to 35% in the CdZnS/ZnS shell. This increase in the Zn content was not accompanied by a decrease of the Cd content, as determined by comparing to the amount of Se which is considered to remain constant throughout the shell additions. This rules out a possible cationic exchange and confirms the effective growth of an additional ZnS layer. According to the EDX analyses, the additional ZnS layer should translate in an volume increase of about 10 %. This increase in volume is however not reflected by an increase in diameter measurable by TEM analysis due to a reshaping of the QDs towards a more spherical shape.

Regarding their optical properties, these QDs with alloyed CdZnS layers are compared together with the starting CdSe/CdS QDs in **Figure 6c-d**. The growth of a CdZnS layer results in a more than 2-fold increase of the absorbance below 500 nm. It also induces a red-shift of both the excitonic absorption and emission peaks. This increase in absorbance and red-shifts are easily explained by the large amount of Cd in the additional layer, as they both are consequences of a larger CdS volume for the same amount of CdSe, allowing the electron to further delocalize in the shell. This also explains the increase in lifetime from 35.1 ns to 45.5 ns (inset **Figure 6d**), due to a lower overlap between the electron and hole wave functions. The growth of an additional ZnS shell on these CdSe/CdS/CdZnS QDs causes again a faint, yet significant, increase in absorption at higher energies and a more pronounced dip on the blue side of the excitonic absorption peak (**Figure 6c**). It also induces a relatively large blue-shift of the emission peak (**Figure 6d**) and a concomitant increase of the lifetime, from 45.5 to 76.1 ns (inset **Figure 6d**). All these observations are in line with those made in the case of CdSe/CdS/ZnS QDs, which confirms the effective growth of the ZnS shell in spite of the limited size increase seen by TEM analyses. Nevertheless, the 7 nm blue-shift of the emission spectrum observed in CdSe/CdS/CdZnS/ZnS QDs (**Figure 6d**) is much more pronounced than in the case of non-alloyed CdSe/CdS/ZnS QDs where the blue-shift was limited to 2 nm (**Figure 4d**). This is truly due to the nature of the alloyed CdZnS layer, as the same observation is made for CdSe/CdZnS/ZnS QDs, *i.e.* when an alloyed CdZnS shell is grown directly on the CdSe cores without any intermediate CdS layer (see the Supporting Information, **Figure S3**). Here again, the blue-shift cannot be attributed to a larger alloying of Zn in the CdZnS layer, because an increased exciton confinement should also translate in a decrease of the lifetime.

Nevertheless, the alloyed layer also benefits the PL efficiency of these QDs. Indeed, the successive shelling with a CdZnS alloy and pure ZnS increases the PLQY from 72% for the starting CdSe/CdS QDs to 73% and then 76%, respectively. Thus, although the increase in PLQY is limited, it is still higher than for the CdSe/CdS/ZnS QDs (74%), and this in spite of the larger QD size, which indicates enhanced surface passivation with minimal additional strain induced, probably thanks to the alloyed layer.

The *Flash* Synthesis for Multi-Shell Nanorods. As mentioned in the introduction, the *flash* synthesis actually originates from the dot-in-rod synthesis reported by Carbone *et al*.[19] These anisotropic structures are obtained by using a mixture of a short and a long phosphonic acids for the dissolution of CdO and stabilization of the NRs. This section will now show that the *flash* procedure can also be used for the growth of a ZnS on these dot-in-rod structures just like in the case of spherical QDs, hence highlighting once again the great versatility of the *flash* technique. However, we have also previously reported that CdSe/CdS NRs synthesized with the protocol of Carbone *et al.* yields NRs which feature physical connections. This was notably evidenced through the silica encapsulation of

these NRs (**Figure 7a**), resulting in many nanoparticles containing two NRs. When primarily attempting to grow a ZnS shell on such CdSe/CdS NRs, the connections remained (**Figure 7b**), which is undesirable for optimal optical properties and application of these NRs. Although the nature and origin of these connection were initially not understood, TEM observations evidenced that some NRs are connected through their sharp tip ends (**Figure 7c**). Since similar ends of these NRs with a non-centrosymmetric wurtzite structure should have the same polarity, this observation rules out the hypothesis of dipolar interactions being at the origin of the connections.

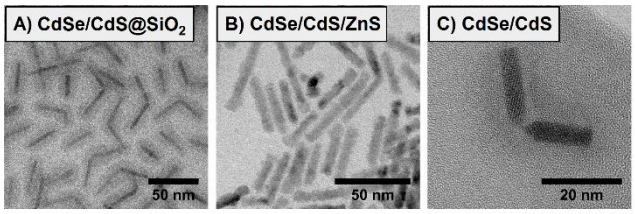

Figure 7. TEM images of a) silica coated CdSe/CdS NRs, b) CdSe/CdS/ZnS NRs grown from connected CdSe/CdS NRs, and c) two CdSe/CdS NRs connected through their tips.

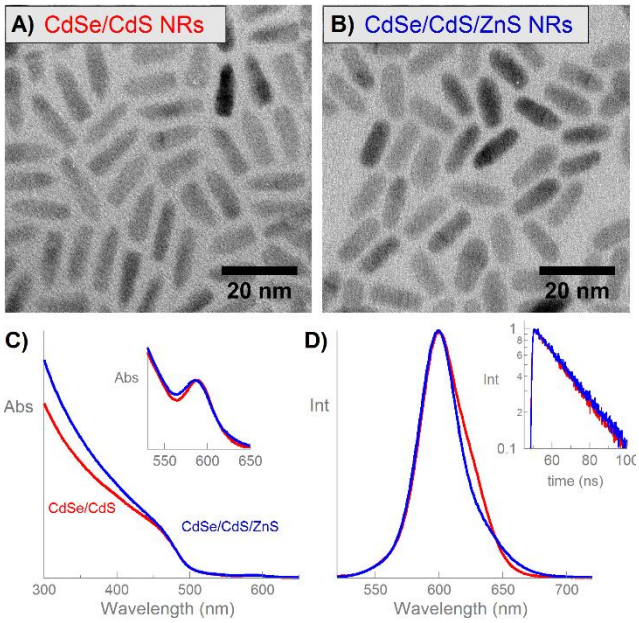

Figure 8. TEM images of a) CdSe/CdS and b) CdSe/CdS/ZnS NRs. Optical properties with c) normalized absorption spectra (inset: focus on the excitonic feature at 590 nm), d) normalized emission spectra (inset: normalized photoluminescence decays of the NRs).

CdSe/CdS NRs. The original CdSe/CdS NRs as reported by Carbone *et al.*[19] were synthesized with a mixture of hexylphosphonic acid (HPA) as the short acid and octadecylphosphonic acid (ODPA) as the long acid. In this work, the short acid was changed for dodecylphosphonic acid (DDPA) and most parameters were adjusted for better standardization with the *flash* procedure. Only few parameters differ from the synthesis of spherical CdSe/CdS QDs. The reaction time for the synthesis of NRs was extended to 8 min as TEM observations have shown substantial growth of the NRs even after 5 min of reaction. The total amount of phosphonic acid was set to the minimal molar ratio of 3:1 compared to the CdO, mostly due to the high cost of these chemicals. The molar ratio ODPA:DDPA was also kept at 1.5, because decreasing this ratio typically caused a destabilization of the NRs during the reaction, indicating that a high amount of the long acid is necessary to preserve the colloidal stability of these relatively large objects, even in spite of increasing the length of the short acid. As for the synthesis of the core CdSe QDs, the use of phosphonic acids for the NRs synthesis can also result in the formation of a phosphonic anhydride polymer and cause gelification of the NRs suspensions. Unfortunately, in this case the use of oleyl alcohol to prevent this was unsuccessful due to formation of an insoluble complex, even at high temperature, with the Cd and ODPA. Thus, to prevent extensive precipitation of a phosphonic acid polymer, the first purification step of the NRs was done while the reaction mixture was still warm as detailed in the experimental section. However, this technique is only efficient for small amount of phosphonic acid in the reaction and the amount of CdSe seeds was therefore limited to 50 nmol for the synthesis of the CdSe/CdS NRs.

Figure 8 shows the TEM image of 5.1 × 15.3 nm CdSe/CdS NRs obtained from the modified synthesis mentioned above, evidencing that the use of DDPA instead of HPA still promotes the growth of an anisotropic shell. More importantly, these NRs are free of connections, as demonstrated through their subsequent silica encapsulation (see the Supporting Information, **Figure S4** for TEM image and experimental details). In the light of this result, it can be reasonably assumed that the tips of the NRs are predominantly passivated by the short chain acid, offering less steric hindrance at these locations and therefore enabling NRs to make direct contact. Once in this situation, the Van der Waals interactions are too strong to allow dissociation of the NRs. Here, the substitution of HPA (6 carbons chain) for DDPA (12 carbons chain) offers better steric passivation to prevent the connections between NRs. Intermediate phosphonic acids with increasing carbon chain lengths have also been tested. The amount of connections between rods decreased with increasing the length of the chain, but only at a carbon chain of 12 did the connections between NRs completely cease to occur.

CdSe/CdS/ZnS NRs. The exact same ZnS shelling procedure as for the spherical QDs was applied to the CdSe/CdS NRs. **Figure 8** shows the TEM images of corresponding CdSe/CdS and CdSe/CdS/ZnS NRs. After this second *flash* step, the NRs grow from 5.1 × 15.3 nm to 5.9 × 15.8 nm, which corresponds to a single monolayer of ZnS. The growth of the ZnS shell was confirmed by EDX analyses which indicated a Zn content of 14 % relatively to the overall composition of the CdSe/CdS/ZnS NRs. This indicates that additional shells can effectively be grown through a *flash* procedure even on these anisotropic structures which are initially passivated with tightly bound phosphonic acids. The seemingly limited growth in the long direction is more likely due to the rounding of the sharp end facets of the NR tips, rather than to an uncomplete ZnS layer. In spite of this rounding, which is an expected consequence of the system reducing the free energy, the NRs virtually retain their aspect ratio, which only decreases from 3 to 2.7. Moreover, **Figure 8b** also evidences that these CdSe/CdS/ZnS NRs, which are now passivated with oleic acid instead of phosphonic acids, are free of connections. This is in clear contrast with those in **Figure 7b**, which highlights the importance of the modification in the CdSe/CdS NR synthesis. This is further demonstrated through the silica encapsulation

of the CdSe/CdS/ZnS NRs (see the Supporting Information, **Figure S4**).

Regarding their optical properties (**Figure 8c** and **d**), the growth of the ZnS shell again increases the absorbance at high energies (**Figure 8c**). However, in contrast with the spherical QDs it does not cause a more pronounced dip after the excitonic feature in the absorption spectrum, nor significantly shifts the emission peak. Even more obvious, the growth of the ZnS does not affect the PL decay of these NRs (inset **Figure 8d**), with measured lifetimes of 20.2 ns and 21.5 ns for the CdSe/CdS and CdSe/CdS/ZnS NRs respectively. On the one hand the lifetime doesn't decrease, indicating that there is virtually no or very limited alloying between the CdS and ZnS shells as this would have increased the overlap between the hole and electron wave functions as previously reported[41] and discussed above. On the other hand, neither did the lifetime increase, as it was the case for spherical QDs. This is also in line with the absence of a strain induced piezoelectric field due to the relatively short diameter of these NRs, even in spite of their anisotropic shape and their long dimension being beyond the Bohr radius of the material. **Figure 8d** shows that the shape of the emission spectrum is affected by the growth of the ZnS shell. The CdSe/CdS NRs feature a small shoulder on the red side of their emission spectrum probably due to NRs with lower aspect ratio and larger diameter as visible in **Figure 8a**. In the CdSe/CdS/ZnS NRs this shoulder is smoothed out towards a more symmetrical spectrum. Although this could be explained by the PLQY of different NRs being affected to different extent by the ZnS shell, this effect is however minor as both samples showed an equal PLQY of 80%.

CONCLUSION

We have developed a generic *flash* method for the formation of a variety of Cd-based core/multiple shell QDs and NRs. The method builds on an improved synthesis of wurtzite CdSe core QDs, where we introduce oleyl alcohol to prevent the polymerization of the phosphonic acid through the formation of a phosphonic ester. This simple change in the reaction allowed for the production of large amounts of high purity core QDs which is key for the subsequent synthesis of high quality core-shell structures. The versatility of the *flash* method is demonstrated through the synthesis of multi-shell QDs and NRs. We have shown that a simple unique procedure can be applied multiple times for the successive growth of not only CdS and ZnS but also CdZnS alloyed shells. This synthesis strategy has proven its efficiency to overcome several limitations for the growth of shells in spite of the lattice mismatch and different surface chemistry. This resulted in materials with enhanced optical properties, even in the case of very thick CdS shells. The high versatility of this technique opens up numerous opportunities for the synthesis of heterostructures covering a wide range of materials beyond those reported here.

ASSOCIATED CONTENT

Supporting information. Characterization of additional samples including TEM images, table with optical properties, absorption and photoluminescent spectra, PL decays. This material is available free of charge via the Internet at http://pubs.acs.org.

AUTHOR INFORMATION

Corresponding Authors

* E-mail: Zeger.Hens@ugent.be

* E-mail: Tangi.Aubert@ugent.be

Notes

The authors declare no competing financial interest.

ACKNOWLEDGMENT

The authors acknowledge European Comission via the Marie-Sklodowska Curie action Phonsi (H2020-MSCA-ITN-642656), BelSPo (IAP 7.35, photonics@be), FWO-Vlaanderen (KaN 1509012N), Ghent University (BOF12/GOA/ (GOA 01G01513; BOF14/PDO/007) and IWT-Vlaanderen for financial support.

REFERENCES

1. Jaiswal, J. K.; Simon, S. M., Potentials and Pitfalls of Fluorescent Quantum Dots for Biological Imaging. *Trends Cell. Biol.* **2004,** 14, (9), 497-504.
2. Chan, W. C. W.; Maxwell, D. J.; Gao, X.; Bailey, R. E.; Han, M.; Nie, S., Luminescent Quantum Dots for Multiplexed Biological Detection and Imaging. *Curr. Opin. Biotechnol.* **2002,** 13, (1), 40-46.
3. McDonald, S. A.; Konstantatos, G.; Zhang, S.; Cyr, P. W.; Klem, E. J.; Levina, L.; Sargent, E. H., Solution-Processed PbS Quantum Dot Infrared Photodetectors and Photovoltaics. *Nat. Mater.* **2005,** 4, (2), 138-142.
4. Lee, S. F.; Osborne, M. A., Brightening, Blinking, Bluing and Bleaching in the Life of a Quantum Dot: Friend or Foe? *Chem. Phys. Chem.* **2009,** 10, (13), 2174-2191.
5. Frantsuzov, P.; Kuno, M.; Jankó, B.; Marcus, R. A., Universal Emission Intermittency in Quantum Dots, Nanorods and Nanowires. *Nat. Phys.* **2008,** 4, (5), 519-522.
6. Heyes, C. D.; Kobitski, A. Y.; Breus, V. V.; Nienhaus, G. U., Effect of the Shell on the Blinking Statistics of Core-Shell Quantum Dots: A Single-Particle Fluorescence Study. *Phys. Rev. B: Condens. Matter* **2007,** 75, (12), 125431-125438.
7. de Mello Donega, C., Synthesis and Properties of Colloidal Heteronanocrystals. *Chem. Soc. Rev.* **2011,** 40, (3), 1512-1546.
8. Eychmüller, A., Structure and Photophysics of Semiconductor Nanocrystals. *J. Phys. Chem. B* **2000,** 104, (28), 6514-6528.
9. Chen, Y.; Vela, J.; Htoon, H.; Casson, J. L.; Werder, D. J.; Bussian, D. a.; Klimov, V. I.; Hollingsworth, J. a., "Giant" Multishell CdSe Nanocrystal Quantum Dots with Suppressed

Blinking. *J. Am. Chem. Soc.* **2008,** 130, 5026-5027.
10. Mahler, B.; Spinicelli, P.; Buil, S.; Quelin, X.; Hermier, J.-P.; Dubertret, B., Towards Non-Blinking Colloidal Quantum Dots. *Nat. Mater.* **2008,** 7, 659-664.
11. Chen, O.; Zhao, J.; Chauhan, V. P.; Cui, J.; Wong, C.; Harris, D. K.; Wei, H.; Han, H. S.; Fukumura, D.; Jain, R. K.; Bawendi, M. G., Compact High-Quality CdSe-CdS Core-Shell Nanocrystals with Narrow Emission Linewidths and Suppressed Blinking. *Nat. Mater.* **2013,** 12, (5), 445-451.
12. Christodoulou, S.; Vaccaro, G.; Pinchetti, V.; De Donato, F.; Grim, J. Q.; Casu, A.; Genovese, A.; Vicidomini, G.; Diaspro, A.; Brovelli, S.; Manna, L.; Moreels, I., Synthesis of Highly Luminescent Wurtzite CdSe/CdS Giant-Shell Nanocrystals Using a Fast Continuous Injection Route. *J. Mater. Chem. C* **2014,** 2, (17), 3439-3447.
13. Nasilowski, M.; Spinicelli, P.; Patriarche, G.; Dubertret, B., Gradient CdSe/CdS Quantum Dots with Room Temperature Biexciton Unity Quantum Yield. *Nano Lett.* **2015,** 15, (6), 3953-3958.
14. Cirillo, M.; Aubert, T.; Gomes, R.; Deun, R. V.; Emplit, P.; Biermann, A.; Lange, H.; Thomsen, C.; Brainis, E.; Hens, Z., "Flash" Synthesis of CdSe/CdS Core−Shell Quantum Dots. *Chem. Mater.* **2014,** 26, 1154-1160.
15. Aubert, T.; Soenen, S. J.; Wassmuth, D.; Cirillo, M.; Deun, R. V.; Braeckmans, K.; Hens, Z., Bright and Stable CdSe/CdS@SiO2 Nanoparticles Suitable for Long-Term Cell Labeling. *ACS Appl. Mater. Interfaces* **2014,** 6, 11714-11723.
16. Xie, W.; Zhu, Y.; Aubert, T.; Hens, Z.; Brainis, E.; Van Thourhout, D., Fabrication and Characterization of On-Chip Silicon Nitride Microdisk Integrated with Colloidal Quantum Dots. *Opt. Express* **2016,** 24, (2), A114-A122.
17. Xie, W.; Zhu, Y.; Aubert, T.; Verstuyft, S.; Hens, Z.; Van Thourhout, D., Low-Loss Silicon Nitride Waveguide Hybridly Integrated with Colloidal Quantum Dots. *Opt. Express* **2015,** 23, (9), 12152-12160.
18. Boldt, K.; Kirkwood, N.; Beane, G. A.; Mulvaney, P., Synthesis of Highly Luminescent and Photo-Stable, Graded Shell CdSe/CdxZn1–xS Nanoparticles by In Situ Alloying. *Chem. Mater.* **2013,** 25, (23), 4731-4738.
19. Carbone, L.; Nobile, C.; De Giorgi, M.; Sala, F. D.; Morello, G.; Pompa, P.; Hytch, M.; Snoeck, E.; Fiore, A.; Franchini, I. R.; Nadasan, M.; Silvestre, A. F.; Chiodo, L.; Kudera, S.; Cingolani, R.; Krahne, R.; Manna, L., Synthesis and Micrometer-Scale Assembly of Colloidal CdSe/CdS Nanorods Prepared by a Seeded Growth Approach. *Nano lett.* **2007,** 7, 2942-2950.
20. Hu, J.; Li, L.; Yang, W.; Manna, L.; Wang, L.; Alivisatos, A. P., Linearly Polarized Emission from Colloidal Semiconductor Quantum Rods. *Science* **2001,** 292, (5524), 2060-2063.
21. Ahmed, S.; Ryan, K. M., Centimetre Scale Assembly of Vertically Aligned and Close Packed Semiconductor Nanorods from Solution. *Chem. Commun.* **2009**, (42), 6421-6423.
22. Aubert, T.; Palangetic, L.; Mohammadimasoudi, M.; Neyts, K.; Beeckman, J.; Clasen, C.; Hens, Z., Large-Scale and Electroswitchable Polarized Emission from Semiconductor Nanorods Aligned in Polymeric Nanofibers. *ACS Photonics* **2015,** 2, (5), 583-588.
23. Diroll, B. T.; Murray, C. B., High-Temperature Photoluminescence of CdSe/CdS Core/Shell Nanoheterostructures. *ACS Nano* **2014,** 8, (6), 6466-6474.
24. Cao, G.; Rabenberg, L. K.; Nunn, C. M.; Mallouk, T. E., Formation of Quantum-Size Semiconductor Particles in a Layered Metal Phosphonate Host Lattice. *Chem. Mater.* **1991,** 3, (1), 149-156.
25. Cao, G.; Lynch, V. M.; Yacullo, L. N., Synthesis, Structural Characterization, and Intercalation Chemistry of Two Layered Cadmium Organophosphonates. *Chem. Mater.* **1993,** 5, (7), 1000-1006.
26. Liu, H.; Owen, J. S.; Alivisatos, A. P., Mechanistic Study of Precursor Evolution in Colloidal Group II-VI Semiconductor Nanocrystal Synthesis. *J. Am. Chem. Soc.* **2007,** 129, (2), 305-312.
27. Owen, J. S.; Chan, E. M.; Liu, H.; Alivisatos, A. P., Precursor Conversion Kinetics and the Nucleation of Cadmium Selenide Nanocrystals. *J. Am. Chem. Soc.* **2010,** 132, (51), 18206-18213.

28. Jasieniak, J.; Smith, L.; Embden, J. v.; Mulvaney, P.; Califano, M., Re-Examination of the Size-Dependent Absorption Properties of CdSe Quantum Dots. *J. Phys. Chem. C* **2009,** 113, (45), 19468-19474.
29. De Geyter, B.; Hens, Z., The Absorption Coefficient of PbSe/CdSe Core/Shell Colloidal Quantum Dots. *Appl. Phys. Lett.* **2010,** 97, (16), 161908-161910.
30. Hens, Z.; Moreels, I., Light Absorption by Colloidal Semiconductor Quantum Dots. *J. Mater. Chem.* **2012,** 22, (21), 10406-10415.
31. de Mello, J. C.; Wittmann, H. F.; Friend, R. H., An Improved Experimental Determination of External Photoluminescence Quantum Efficiency. *Adv. Mater.* **1997,** 9, (3), 230-232.
32. Connell, M. A.; Bowyer, P. J.; Adam Bone, P.; Davis, A. L.; Swanson, A. G.; Nilsson, M.; Morris, G. A., Improving the Accuracy of Pulsed Field Gradient NMR Diffusion Experiments: Correction for Gradient Non-Uniformity. *J. Magn. Reson.* **2009,** 198, (1), 121-131.
33. Sinnaeve, D., The Stejskal-Tanner Equation Generalized for Any Gradient Shape-An Overview of Most Pulse Sequences Measuring Free Diffusion. *Concepts Magn. Reson.* **2012,** 40A, (2), 39-65.
34. Hens, Z.; Martins, J. C., A Solution NMR Toolbox for Characterizing the Surface Chemistry of Colloidal Nanocrystals. *Chem. of Mater.* **2013,** 25, 1211-1221.
35. De Roo, J.; Van Driessche, I.; Martins, J. C.; Hens, Z., Colloidal Metal Oxide Nanocrystal Catalysis by Sustained Chemically Driven Ligand Displacement. *Nat. Mater.* **2016,** 15, (5), 517-21.
36. Gomes, R.; Hassinen, A.; Szczygiel, A.; Zhao, Q.; Vantomme, A.; Martins, J. C.; Hens, Z., Binding of Phosphonic Acids to CdSe Quantum Dots: A Solution NMR Study. *J. Phys. Chem. Lett.* **2011,** 2, (3), 145-152.
37. De Roo, J.; Van den Broeck, F.; De Keukeleere, K.; Martins, J. C.; Van Driessche, I.; Hens, Z., Unravelling the Surface Chemistry of Metal Oxide Nanocrystals, the Role of Acids and Bases. *J. Am. Chem. Soc.* **2014,** 136, (27), 9650-9657.
38. Kopping, J. T.; Patten, T. E., Identification of Acidic Phosphorus-Containing Ligands Involved in the Surface Chemistry of CdSe Nanoparticles Prepared in Tri-N-Octylphosphine Oxide Solvents. *J. Am. Chem. Soc.* **2008,** 130, (17), 5689-5698.
39. Morris-Cohen, A. J.; Donakowski, M. D.; Knowles, K. E.; Weiss, E. A., The Effect of a Common Purification Procedure on the Chemical Composition of the Surfaces of CdSe Quantum Dots Synthesized with Trioctylphosphine Oxide. *J. Phys. Chem. C* **2010,** 114, (2), 897-906.
40. Rabouw, F. T.; Kamp, M.; van Dijk-Moes, R. J.; Gamelin, D. R.; Koenderink, A. F.; Meijerink, A.; Vanmaekelbergh, D., Delayed Exciton Emission and Its Relation to Blinking in CdSe Quantum Dots. *Nano Lett.* **2015,** 15, (11), 7718-7725.
41. Diroll, B. T.; Turk, M. E.; Gogotsi, N.; Murray, C. B.; Kikkawa, J. M., Ultrafast Photoluminescence from the Core and the Shell in CdSe/CdS Dot-in-Rod Heterostructures. *Chem. Phys. Chem.* **2016,** 17, (5), 759-765.
42. Christodoulou, S.; Rajadell, F.; Casu, A.; Vaccaro, G.; Grim, J. Q.; Genovese, A.; Manna, L.; Climente, J. I.; Meinardi, F.; Raino, G.; Stoferle, T.; Mahrt, R. F.; Planelles, J.; Brovelli, S.; Moreels, I., Band Structure Engineering via Piezoelectric Fields in Strained Anisotropic CdSe/CdS Nanocrystals. *Nat. Commun.* **2015,** 6, 7905-7913.
43. Meinardi, F.; Colombo, A.; Velizhanin, K. A.; Simonutti, R.; Lorenzon, M.; Beverina, L.; Viswanatha, R.; Klimov, V. I.; Brovelli, S., Large-Area Luminescent Solar Concentrators Based on 'Stokes-Shift-Engineered' Nanocrystals in a Mass-Polymerized PMMA Matrix. *Nat. Photonics* **2014,** 8, (5), 392-399.
44. Bronstein, N. D.; Li, L.; Xu, L.; Yao, Y.; Ferry, V. E.; Alivisatos, A. P.; Nuzzo, R. G., Luminescent Solar Concentration with Semiconductor Nanorods and Transfer-Printed Micro-Silicon Solar Cells. *ACS Nano* **2014,** 8, (1), 44-53.

Supporting Information for

Revisited Wurtzite CdSe Synthesis : a Gateway for the Versatile Flash Synthesis of Multi-Shell Quantum Dots and Rods

Emile Drijvers[1,3], Jonathan De Roo[2], Krisztina Fehér[4], Zeger Hens[1,3] and Tangi Aubert[1,3]

[1] Physics and Chemistry of Nanostructures (PCN), and [2] Sol-gel Centre for Research on Inorganic Powders and Thin films Synthesis (SCRiPTS), Department of Inorganic and Physical Chemistry, Ghent University, Krijgslaan 281-S3, 9000 Ghent, Belgium.

[3] Center for Nano and Biophotonics (NB-Photonics), Ghent University, Sint-Pietersnieuwstraat 41, 9000 Ghent, Belgium.

[4] NMR and Structure Analysis Unit, Department of Organic and Macromolecular Chemistry, Ghent University, Krijgslaan 281-S4, 9000 Ghent, Belgium.

KEYWORDS: Semiconductor, nanocrystal, NMR, CdSe/CdS/ZnS, giant core-shell.

Corresponding authors: Zeger.Hens@UGent.be, Tangi.Aubert@UGent.be

Content: Additional TEM images, table of optical properties, absorption and photoluminescent spectra, photoluminescent decays.

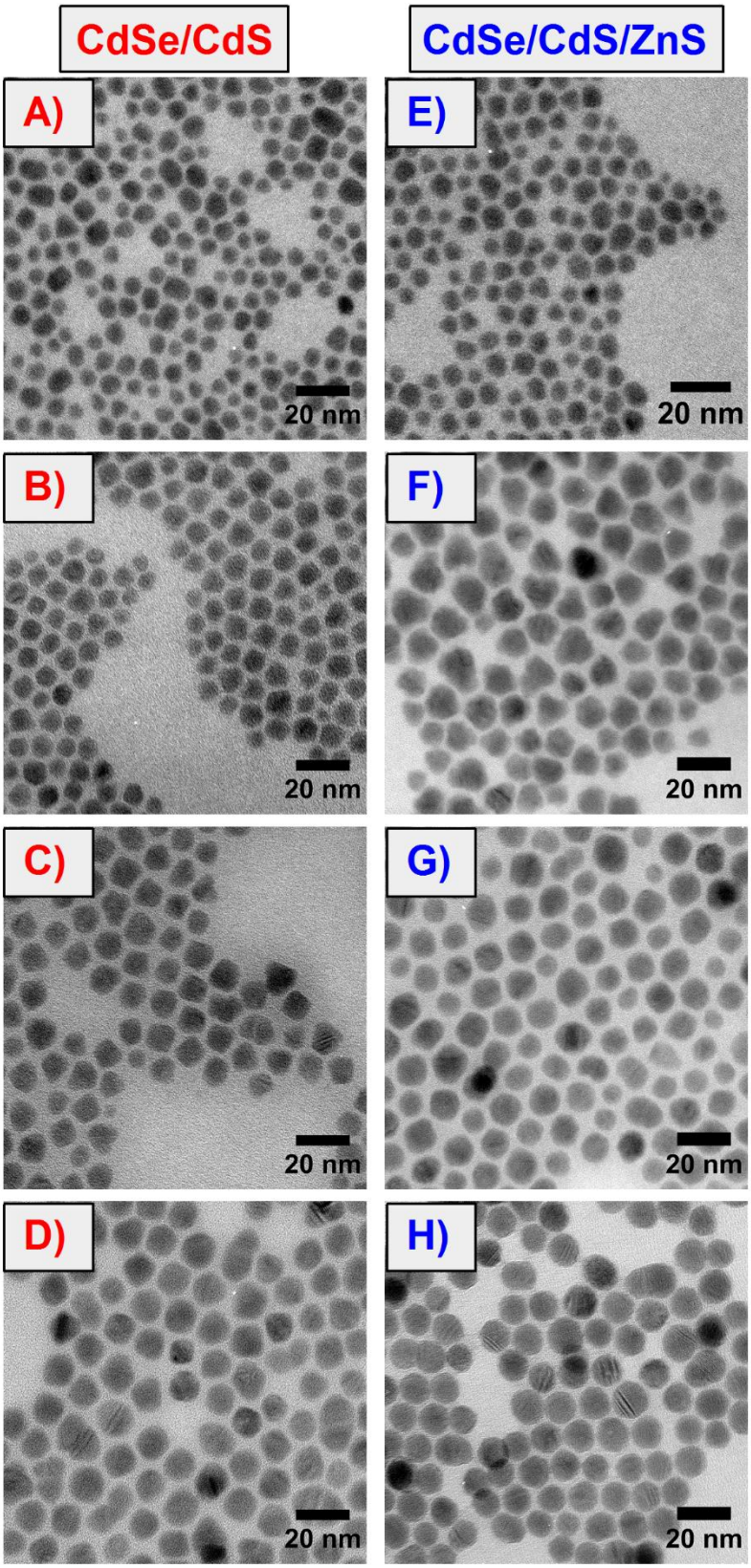
CdSe/CdS
CdSe/CdS/ZnS
A)
E)
B)
F)
C)
G)
D)
H)
20 nm

Figure S1. TEM images of a) CdSe/CdS QDs of 5.0 ± 0.9 nm, b) 8.5 ± 1.2 nm, c) 9.9 ± 1.6 nm and d) 13.4 ± 2.0 nm produced from the same 3 nm CdSe cores via the *flash* synthesis. TEM images of e) CdSe/CdS/ZnS QDs of 6.8 ± 1.0 nm, f) 10.9 ± 1.5 nm, g) 11.3 ± 1.3 nm and h) 14.0 ± 1.5 nm grown from a), b), c) and d) respectively.

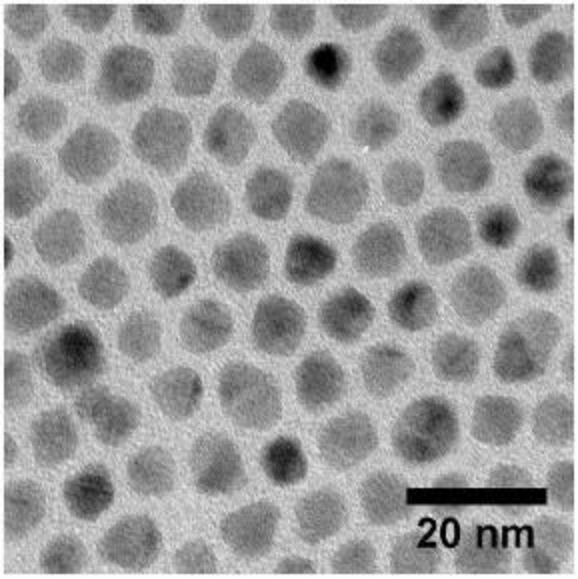

Figure S2. TEM images of core-shell CdSe/CdS QDs with size dispersions below 10% when increasing the concentration of the seeds from 200 nmol to 400 nmol in the *flash* synthesis.

Table S1. Overview of properties of core-shell QDs with different sizes.

Sample	Seeds used	Composition	Diameter (nm)	ZnS thickness (nm)	Emission (nm)	PLQY (%)
QD 2	3 nm CdSe	CdSe/CdS	5.0 ± 0.9	-	586	48
QD 3	QD 2	CdSe/CdS/ZnS	6.8 ± 1.0	0.9	587	51
QD 4	3 nm CdSe	CdSe/CdS	8.5 ± 1.2	-	615	67
QD 5	QD 4	CdSe/CdS/ZnS	10.9 ± 1.5	1.2	614	68
QD 6	3 nm CdSe	CdSe/CdS	9.9 ± 1.6	-	622	60
QD 7	QD 6	CdSe/CdS/ZnS	11.3 ± 1.3	0.7	617	72
QD 8	3 nm CdSe	CdSe/CdS	13.4 ± 2.0	-	622	36
QD 9	QD 8	CdSe/CdS/ZnS	14.0 ± 1.5	0.3	620	47

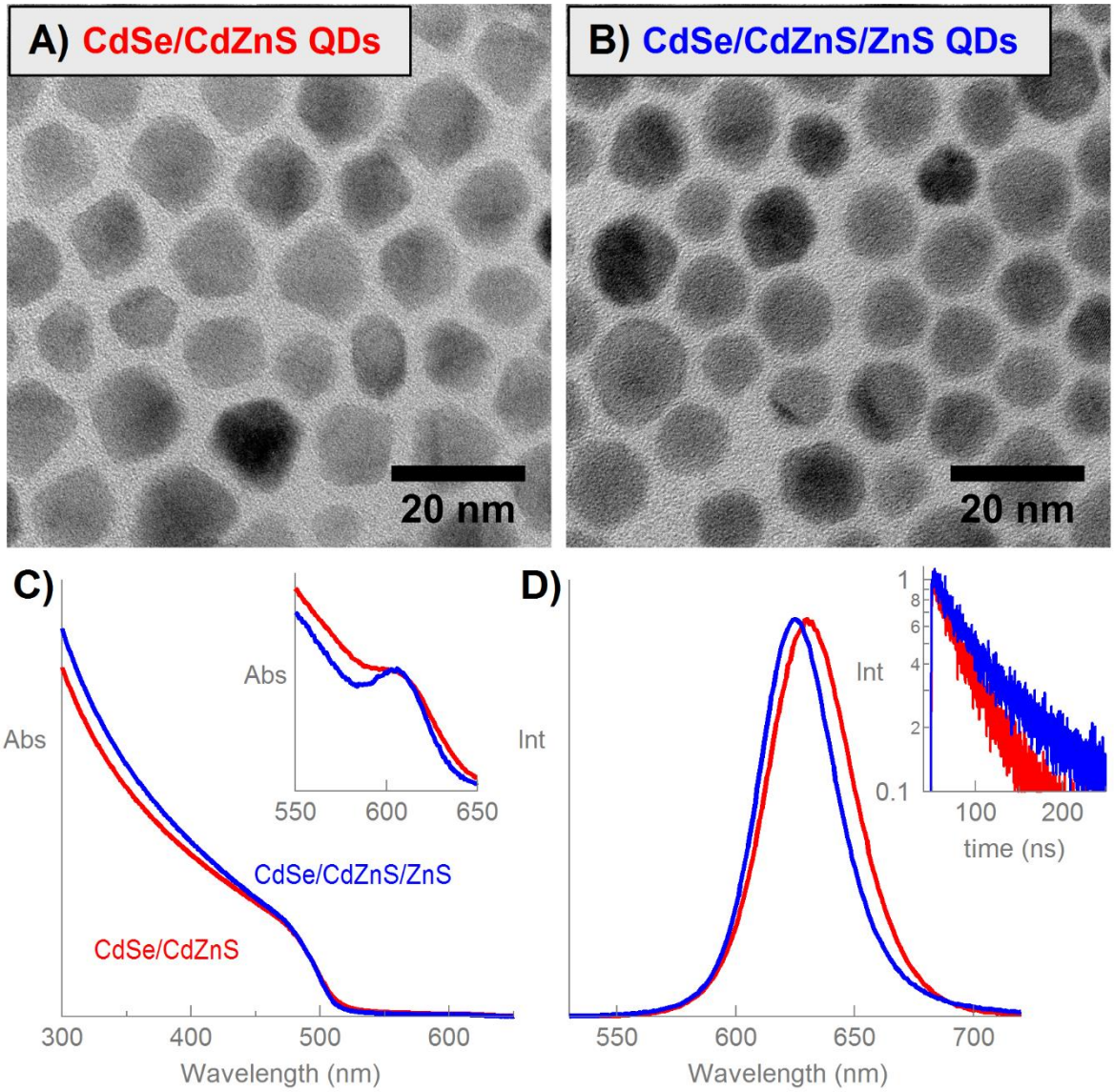

Figure S3. TEM images of a) CdSe/CdZnS and b) CdSe/CdZnS/ZnS QDs. Optical properties with c) normalized absorption spectra (inset: focus on the excitonic feature at 600 nm), d) normalized emission spectra (inset: normalized photoluminescence decays of the QDs).

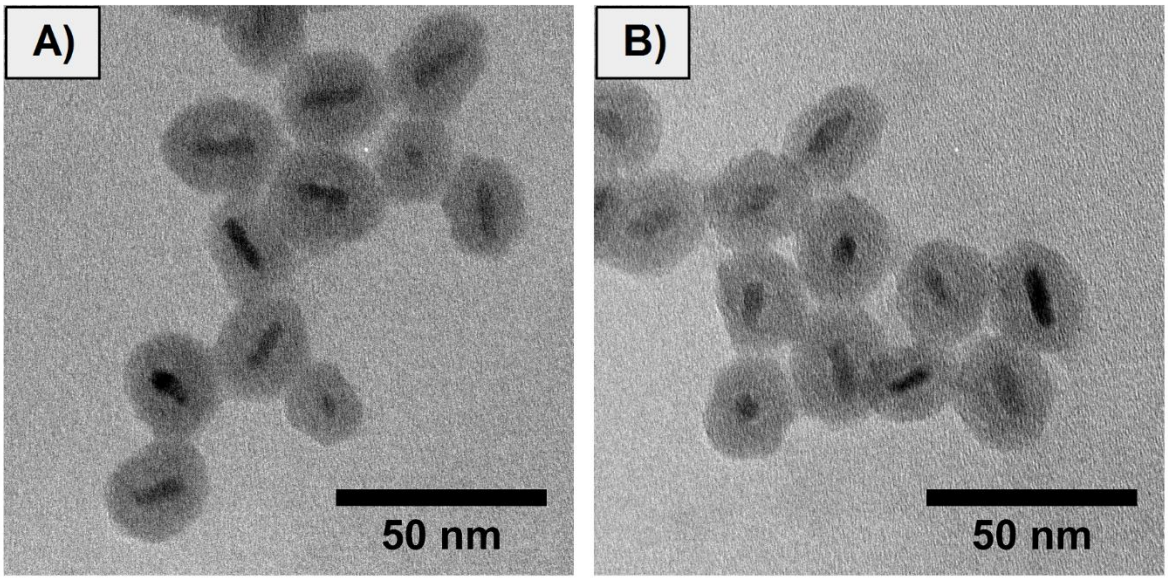

Figure S4. TEM images of a) CdSe/CdS NRs and b) CdSe/CdS/ZnS NRs encapsulated in a silica matrix which display no tip-to-tip connections. The NRs were encapsulated in a silica matrix through a water-in-oil microemulsion process according to a procedure described in the literature.[15] Briefly, 0.2 nmol of NRs was mixed to 2 mL of heptane and 640 µL of surfactant (Brij30). After 15 minutes of stirring 110 µL of 3% ammonia solution in Milli-Q water was added to the mixture. After 1 hour of stirring, 25 µL of tetraethyl orthosilicate (TEOS) was added. The reaction was stopped after 3 day by adding 2 mL of EtOH in order to destabilize the microemulsion. The nanoparticles were collected by centrifugation and purified by repeated centrifugation in EtOH and two times in Milli-Q water. The particles were stored in Milli-Q water.

TOC graphic